92-17

SIGNAL PROCESSING VI
THEORIES AND APPLICATIONS

Proceedings of EUSIPCO-92
Sixth European Signal Processing Conference
Brussels, Belgium, August 24–27, 1992

Edited by

J. VANDEWALLE
ESAT Laboratory
Katholieke Universiteit Leuven
Heverlee, Belgium

R. BOITE
Département E.P.I.
Faculté Polytechnique de Mons
Mons, Belgium

M. MOONEN
A. OOSTERLINCK
ESAT Laboratory
Katholieke Universiteit Leuven
Heverlee, Belgium

VOLUME III





1992

ELSEVIER
AMSTERDAM • LONDON • NEW YORK • TOKYO

IMPROVED QUANTITATIVE TIME-DOMAIN ANALYSIS OF NMR DATA BY TOTAL LEAST SQUARES.

S. Van Huffel[1], L. Aerts, J. Bervoets, J. Vandewalle, C. Decanniere[2], P. Van Hecke[2]

ESAT Laboratory, Dept. of Electrical Engineering, Katholieke Universiteit Leuven, Belgium.
[2]Biomedical NMR Unit, Faculty of Medicine, Katholieke Universiteit Leuven, Belgium.

Abstract. Experiments show that the use of Total Least Squares (TLS) instead of Least Squares (LS) in linear prediction and state-space methods, two time-domain fitting methods for Nuclear Magnetic Resonance (NMR) data, improves the accuracy of all NMR parameter estimates for any number of data points considered. In particular, the damping factors benefit from the use of TLS especially when the peak Signal-to-Noise Ratio (SNR) is low thereby also improving the accuracy of the amplitudes and phases.

1. INTRODUCTION.

The TLS problem [9] has been devised as a more global fitting method than the LS problem for solving overdetermined sets of linear equations $AX \approx B$ when all measurements in B, as well as in A, are subject to errors.
TLS definition. Given complex matrices $A_{m\times n}$ and $B_{m\times d}$, $m \geq n$, then the following problem:

$$\begin{array}{ll} \text{minimize} & \| [A;B] - [\hat{A};\hat{B}] \|_F \text{ over all } [\hat{A};\hat{B}]_{m\times(n+d)} \\ \text{subject to} & \text{Range}(\hat{B}) \subseteq \text{Range}(\hat{A}) \end{array}$$

is called the *TLS problem* ($\|.\|_F$ denotes the Frobenius norm). If $[\hat{A};\hat{B}]$ solves this problem, then any X satisfying $\hat{A}X = \hat{B}$ is called a *TLS solution* of $AX \approx B$.
In particular, if A, B are observations of an exact relationship $A_0X_0 = B_0$ and the errors are uncorrelated with zero mean and equal variance, TLS is able to compute a strongly consistent, asymptotically unbiased estimate of the true parameters X_0. The LS solution is always inconsistent and biased in this case. This consistency property is fairly well approximated in moderately sized problems [9]. In many applications where these error conditions are approximately satisfied, the TLS solution has been proven to be more accurate than the LS solution (see [9] for a list of references). Here we investigate the use of TLS in the quantitative analysis of NMR data.

2. METHODS.

Model. Consider the case where N uniformly sampled data points are fitted to the time-domain model function:

$$y_n = \sum_{k=1}^{K} c_k z_k^{n+\delta} = \sum_{k=1}^{K} (a_k e^{j\phi_k}) e^{(-d_k + j2\pi f_k)(n+\delta)\Delta t} \qquad (1)$$

where $n = 0, \ldots, N-1$ and $j = \sqrt{-1}$. Δt is the constant sampling interval and $\delta\Delta t$ is the time lapse between the effective time origin and the first sample. The objective is to estimate the frequencies f_k, damping factors d_k, amplitudes a_k and phases ϕ_k, $k = 1, \ldots, K$.

Linear Prediction. These parameters can be estimated by the Kumaresan-Tufts' *linear prediction* (LP) method combined with SVD [5], called LPSVD in NMR [2]. The LP equations for backward prediction using complex conjugate data are written in matrix form as $H_{(N-M)\times M}p \approx h_0$ where $M \geq K$ is the prediction order. Truncating the SVD of H to rank K and computing the minimum norm LS solution $\hat{p}$ gives the coefficients of the prediction polynomial $1 - \sum_{k=1}^{M} \hat{p}_k z^{-k}$. The estimates $\hat{z}_k = e^{\hat{s}_k}$ of the complex signal poles $z_k, k = 1, \ldots, K$ in (1), which contain the frequency and damping factor estimates $\hat{f}_k$ and $\hat{d}_k$, are then derived from the K largest (in absolute value) roots r_k of the prediction polynomial, called *signal zeros* and given by $r_k = e^{-\hat{s}_k} = e^{\hat{d}_k + j2\pi\hat{f}_k}$. Truncating instead the SVD of $[H; h_0]$ to rank K and computing the *minimum norm TLS* solution results in the TLS based LP method [7], called LPTLS here. Although LPSVD and LPTLS yield identical estimates to a first order perturbation approximation (i.e. for high SNR) [4], they behave quite differently at low SNR (see further).
Once the $\hat{z}_k$ are known the complex-valued linear parameters c_k, which contain the amplitudes a_k and phases ϕ_k, are estimated as the LS solution of a set $Ac \approx b$ obtained by fitting the N model equations (1) to the data points (where the z_k are replaced by the computed estimates $\hat{z}_k$). It should be noted that here the use of TLS is not recommended since the errors introduced in A are systematic and not at all random or equally sized.

State-space based methods. Kung's state-space approach combined with SVD [6], known as HSVD in NMR

[1]Research Associate of the Belgian N.F.W.O. (National Fund for Scientific Research)

[3], is a better alternative to the LP methods since it circumvents the steps of polynomial rooting and root selection. It is based on the fact that the N data points y_n in (1) can be modeled by an autonomous linear state-space model of dimension K:

$$\begin{aligned} x_{n+1} &= Ax_n \qquad x_n \text{ complex state vector} \\ y_n &= Cx_n \qquad C \text{ complex row vector} \end{aligned} \tag{2}$$

Equating (1) and (2) yields $y_n = CA^n x_0 = \sum_{k=1}^{K} c_k z_k^n$ (assume $\delta = 0$) defining the state-space matrices $A = \mathrm{diag}(z_1, \ldots, z_K)$, $x_0 = [1, \ldots, 1]^T$ and $C = [c_1, \ldots, c_K]$. Combining the N data points in a Hankel matrix H and using $y_n = CA^n x_0$ decomposes $H = \mathcal{O}\mathcal{C}$ in an observability matrix $\mathcal{O}$ and a controllability matrix $\mathcal{C}$ given by:

$$H = \begin{bmatrix} y_0 & \cdots & y_{M-1} \\ \vdots & \ddots & \vdots \\ y_{N-M} & \cdots & y_{N-1} \end{bmatrix} = \begin{bmatrix} C \\ CA \\ \vdots \\ CA^{N-M} \end{bmatrix} [x_0 \; Ax_0 \ldots A^{M-1}x_0] \tag{3}$$

$\mathcal{O}$ and $\mathcal{C}$ can be computed up to a similarity transformation S from the truncated SVD of the rank K matrix H:

$$H = (\mathcal{O}S^{-1})(S\mathcal{C}) = U_K \Sigma_K V_K^H = \hat{U}_K \hat{V}_K^H \tag{4}$$

where $\hat{U}_K = U_K$ (resp., $U_K \Sigma_K^{\frac{1}{2}}$) and $\hat{V}_K = V_K \Sigma_K$ (resp., $V_K \Sigma_K^{\frac{1}{2}}$) if an *unbalanced* (resp., *balanced*) splitting is used. The similarity transformation matrix S is computed by taking into consideration that the system matrix A in (2) is diagonal and the first column of the matrix $\mathcal{C}$ is given by $x_0 = [1, \ldots, 1]^T$. Hereto, write S as TD where D is diagonal and substitute in (3-4) yielding:

$$H = \begin{bmatrix} CD^{-1}T^{-1} \\ CD^{-1}T^{-1}Q \\ \vdots \\ CD^{-1}T^{-1}Q^{N-M} \end{bmatrix} [TDx_0 \; QTDx_0 \ldots Q^{M-1}TDx_0] \tag{5}$$

where $Q = SAS^{-1}$ has the same eigenvalues as A. By equating the first right-hand side term of (5) with $\hat{U}_K$ in (4), Q follows immediately from solving:

$$\underline{\hat{U}}_K Q = \bar{\hat{U}}_K \tag{6}$$

where $\underline{\hat{U}}_K$ (resp., $\bar{\hat{U}}_K$) is obtained from $\hat{U}_K$ by deleting its last (resp., first) row. Since we use noisy data the set (6) is not compatible. Solving (6) with LS results in the HSVD algorithm. If an unbalanced splitting is used, this can be done very efficiently using the Sherman-Morrison formula [3,6]. Since both sides of (6) are noisy we could as well solve (6) *with TLS* resulting in the HTLS algorithm. Once Q is estimated its eigenvalues give the signal pole estimates $\hat{z}_k$ yielding the desired $\hat{f}_k$ and $\hat{d}_k$.

Once the $\hat{z}_k$ are known, HSVD and HTLS estimate the c_k (which contain the a_k and ϕ_k) by a LS fit of the model Eqs. (1) to the data (cfr. the LP methods).

The c_k can also be estimated *directly* from the state-space model setting as follows. Since $Q = SAS^{-1} = TAT^{-1}$, T is given by the eigenvector matrix of Q. Multiplying the first column $\hat{v}_1$ of $\hat{V}_K^H$ with T^{-1} yields $d = T^{-1}\hat{v}_1 = Dx_0$. Hence $D = \mathrm{diag}(d_1, \ldots, d_K)$. If $\hat{u}_1^T$ denotes the first row of $\hat{U}_K$ then $C = [c_1, \ldots, c_K]$ is estimated by $\hat{u}_1^T TD$. The algorithm that solves (6) by TLS but estimates the c_k directly as above is called HCOP here.

3. RESULTS.

The following example is given to illustrate the improvement in accuracy that may accrue from the use of TLS in the modeling problem defined by (1).

Example: N data points, uniformly sampled at 10 kHz (i.e. $\Delta t = 10^{-4}s$), are exactly modeled by a fifth order model function (1) given in Table 1 and Fig. 1. These data points are perturbed by white Gaussian noise whose real and imaginary components have standard deviation σ_ν. (Relative) Root Mean-Squared Error (RMSE) values of the estimates of all signal parameters f_k, d_k, a_k and ϕ_k are computed using 200 noise realizations (excluding failures) at each considered σ_ν. A *failure* occurs if *not all peaks are resolved* within specified intervals lying symmetrically around the exact frequencies. The halfwidth of the intervals are respectively 82,82,82,43 and 82 and are derived from the CR bounds at the noise standard deviation where the intervals of peak 4 and 5 are coinciding. Varying σ_ν and number of data points N are considered. Unless stated otherwise, the estimated model order K is set to 5 and $\delta = 0$ in (1). The Cramér-Rao (CR) lower bounds are derived from the exact parameter values and σ_ν. The SNR at peak k is defined by $10\log(a_k^2/(2\sigma_\nu^2))$. This example describes a typical in vivo ^{31}P NMR signal [2,3] where a lot of spectral peaks are to be resolved us-

peak k	f_k (Hz)	d_k (Hz)	a_k (a.u.)	ψ_k (deg.)
1	-1379	208	6.1	15
2	-685	256	9.9	15
3	-271	197	6.0	15
4	353	117	2.8	15
5	478	808	17.0	15

Table 1: Exact parameter values of the example. a.u. means arbitrary units and $\psi_k = \phi_k * 180/\pi$ expresses the phase in degrees.

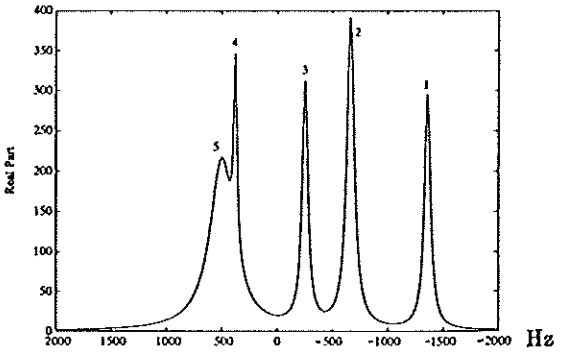


Figure 1: FFT of the exact signal (real part).

ing a limited number of noisy observations. Usually, the signal frequencies are known a priori but the damping factors, amplitudes and phases need to be computed as accurately as possible in order to determine the concentrations of the chemical components of interest.

LP methods. In the absence of noise the desired signal zeros $r_k = e^{d_k + j2\pi f_k}$ fall outside the unit circle while the remaining $M - K$ extraneous zeros lie inside the unit circle [5]. However, if the SNR is low or the data are truncated, extraneous zeros may occasionally fall outside the unit circle whereas signal zeros may fall inside the unit circle. In these cases, LPTLS as well as LPSVD have a tendency to miss relevant spectral peaks. However, LPTLS systematically recovers a higher proportion of the spectral peaks than LPSVD, as experimentally observed [1,8] and shown in Table 2.

N=100	0.75	1.00	1.25	1.50	1.75	2.00
LPSVD	6(6)	24(24)	40(33)	79(60)	120(94)	154(127)
LPTLS	5(5)	22(22)	29(23)	63(48)	99(75)	140(110)
N=128	0.75	1.00	1.25	1.50	1.75	2.00
LPSVD	0(0)	0(0)	4(4)	19(17)	54(39)	88(55)
LPTLS	0(0)	0(0)	6(6)	16(13)	48(30)	83(46)

Table 2: Number of times (out of 200) that LPSVD and LPTLS fail to resolve the 5 peaks of the example within the specified frequency intervals (between brackets: fail to find 5 zeros r_k outside the unit circle) for $N = 100$ and 128 at different σ_ν (from 0.75 to 2.0).

If one overestimates the model order K then clearly more signal zeros fall outside the unit circle. But also here it was observed that LPTLS resolves the difficult peaks (e.g. peak 4 in the example) more often than LPSVD. In our experiments the prediction order M was set to $\frac{3}{4}N$, which is considered to provide the best parameter accuracy [2,4,5]. At that prediction order the differences in resolution and accuracy between the LPSVD and LPTLS estimates of all parameters f_k, d_k, a_k, ϕ_k corresponding to resolved peaks are rather small compared to lower prediction orders (e.g. $M = \frac{1}{3}N \geq K$) where the superior performance of LPTLS compared to LPSVD is more pronounced (as shown in [7,8]). Especially the damping factors benefit from the use of TLS particularly when the peak SNR is low. That's also the reason why LPTLS has less failures since the damping factor determines whether or not the signal zero falls outside the unit circle.

State-space based methods. In general, those methods are computationally more efficient and provide more accurate parameter estimates than the LP methods. The data matrix H in (3) is taken as square as possible since then the best parameter accuracy is obtained [3] (although the minimum is very flat [1]), i.e. $M = N/2$. It was observed that HSVD and HTLS have (approximately) the same failure rate (increasing from $\leq$ 1% below $\sigma_\nu = 1.4$ to 32% and 45% at $\sigma_\nu = 2.0$ for $N = 128$ and 100 respectively), probably because the failure rate mainly depends on the quality of the signal subspace estimate $\hat{U}_K$ which is the same for HSVD and HTLS. Note that the occurrence of a failure is always due to the fact that peak 4 and 5 are fitted by only one peak while an additional noise peak appears mostly far away from the exact frequencies (often around $\pm$4000 Hz).

k	Method	f_k (Hz)	d_k (Hz)	a_k (a.u.)	ψ_k (deg.)
4	HSVD	-2.797 $\pm$10.45	40.47 $\pm$77.55	0.829 $\pm$1.590	8.562 $\pm$21.36
4	HTLS	-0.598 $\pm$10.04	14.48 $\pm$61.03	0.487 $\pm$1.195	2.316 $\pm$21.15
5	HSVD	7.528 $\pm$20.22	42.60 $\pm$166.2	-0.421 $\pm$1.954	-2.562 $\pm$8.681
5	HTLS	4.974 $\pm$20.02	-14.34 $\pm$100.3	-0.399 $\pm$1.982	-0.704 $\pm$6.398

Table 3: Bias$\pm$standard deviation values of the parameter estimates of peak 4 and 5 of the example. $N = 128$ and $\sigma_\nu = 1.5$.

Although the use of TLS does not improve the resolution of closely spaced peaks it certainly *improves the accuracy* of the parameter estimates whenever the peaks are resolved. It was observed that the use of TLS only slightly improves the accuracy of the frequency estimates (about 2-3 Hz for peak 4 and 5 for varying σ_ν) but, in contrast, the damping factor estimates and consequently also the amplitude and phase estimates benefit significantly from the use of TLS. Especially the bias decreases considerably while the variance of the HTLS estimates is somewhat lower than that of the HSVD estimates, as shown in Table 3. The differences in accuracy improvement are most pronounced for the difficult peaks 4 and 5 (with low SNR), as shown in Fig. 2. For isolated peaks (e.g. 1, 2 and 3 in Fig. 1) the differences in accuracy are marginal. These improvements in accuracy due to the use of TLS are apparent at any number of data points N varying from 60 to 240 (the signal dies out around $N = 128$), as shown in Fig. 3. Note that the failure rate can be improved significantly by overestimating the model order (e.g. at $\sigma_\nu = 2$ for $N = 128$ the failure rate decreases below 15% for $K = 6$ and below 9% for $K = 8$) but the differences in accuracy between HTLS and HSVD remain relatively the same.

As shown in Fig. 2(b) and (c) no significant differences in accuracy have been observed between HCOP that computes the amplitude and phase estimates directly from the state-space model setting and HTLS that computes the estimates from a LS fit to the data. Only at low SNR HCOP tends to be slightly less accurate than HTLS. Since Σ_K and V_K are always available from the SVD of H in (3), HCOP is computationally more efficient than HTLS.

Similar observations are made for differently sized data matrices H provided $0.4 \leq \frac{M}{N} \leq 0.6$. Outside this region the errors (may) increase significantly. Finally, it should

be noted that no differences in accuracy have been observed between balanced and unbalanced splitting.

REFERENCES.

[1] Aerts, L. and Bervoets, J., Master's thesis, Dept. of Electr.Eng., K.U.Leuven, 1991.

[2] Barkhuijsen, H., De Beer, R., Bovée, W.M.M.J. and Van Ormondt, D., J. Magn. Res. 61 (1985) 465.

[3] De Beer, R. and Van Ormondt, D., *Analysis of NMR data using time-domain fitting procedures*, in: Rudin, M. (ed.), NMR Basic Principles and Progress, Vol.26 (Springer-Verlag,Berlin Heidelberg,1992) pp.201-248.

[4] Hua, Y. and Sarkar, T.P., IEEE Trans. ASSP 38 (1990) 2004.

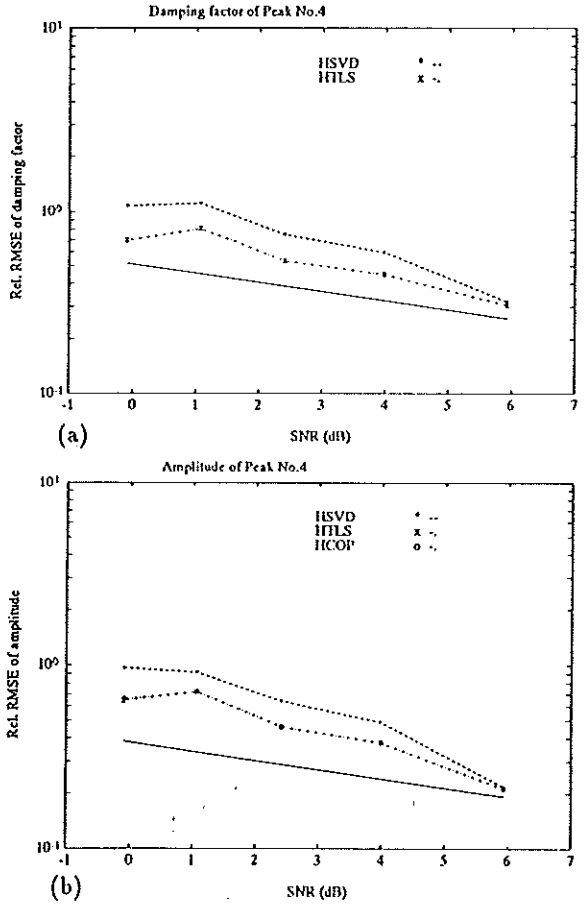
[5] Kumaresan, R. and Tufts, D.W., IEEE Trans. ASSP 30 (1982) 833.

[6] Kung, S.Y., Arun, K.S. and Rao, D.V.B., J. Opt. Soc. Am. 73 (1983) 1799.

[7] Rahman, M.D.A. and Yu, K.B., IEEE Trans. ASSP 35 (1987) 1440.

[8] Tirendi, C.F. and Martin, J.F., J. Magn. Res. 85 (1989) 162.

[9] Van Huffel, S. and Vandewalle, J., *The total least squares problem: computational aspects and analysis* (Frontiers in Appl.Math.9, SIAM, Philadelphia, 1991).



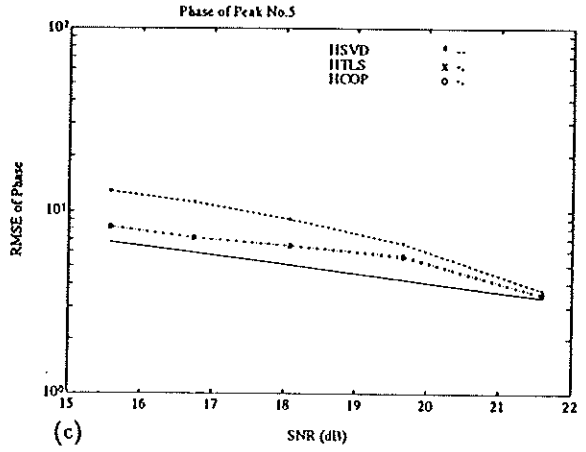


Figure 2: (Relative) RMSE values of the estimated (a) damping factor $\hat{d}_4$, (b) amplitude $\hat{a}_4$ and (c) phase $\hat{\phi}_5$ versus the corresponding peak SNR. N=128. The solid line is the CR bound.

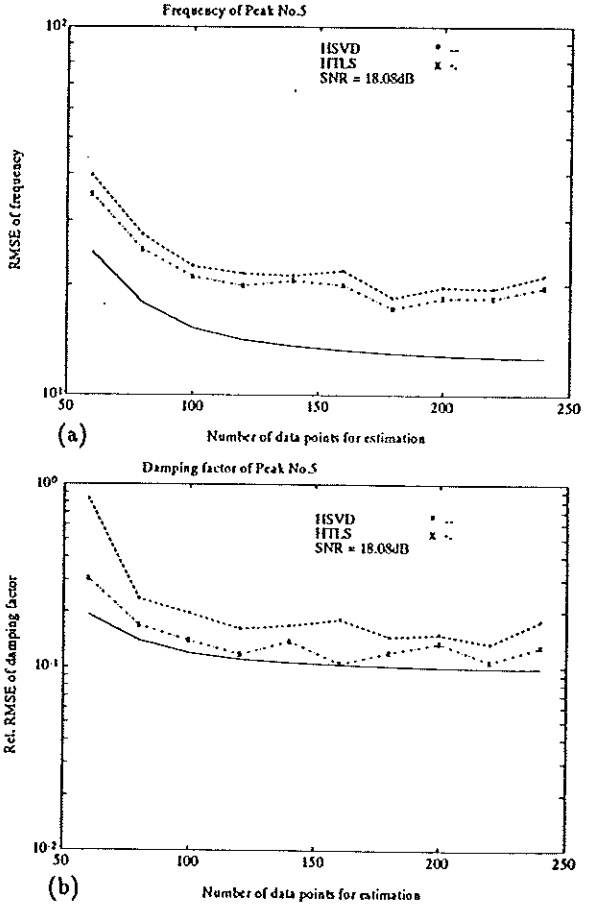


Figure 3: (Relative) RMSE values of the estimated (a) frequency $\hat{f}_5$ (b) damping factor $\hat{d}_5$ at $\sigma_\nu = 1.5$ versus the number of data points. The solid line is the CR bound.